Frequency-dependent transversal flow control in centrifugal microfluidics

Thilo Brenner, Thomas Glatzel, Roland Zengerle and Jens Ducrée

This work presents a novel flow switch for centrifugal microfluidic platforms which is solely controlled by the Coriolis pseudo force. This Coriolis switch consists of an inverse Y-structure with one common upstream channel and two symmetric outlets on a rotating disk. Above a certain threshold frequency, the Coriolis force becomes dominant that the entire flow is diverted into one of the outlets which is selected by the direction of rotation. The threshold frequency has been measured to be 350 rad s^{-1} (~ 55.7 Hz) for a channel width of 360 μm and a depth of 125 μm. The results are supported by extensive CFD simulations.

1. Introduction

Rotating disks have been introduced as convenient platforms for liquid handling in microfluidics.[1–6] Liquids on a disk are easily pumped from the center to the outer perimeter by the centrifugal force which creates an artificial gravity in the rotating disk frame. This approach circumvents complex integration of actuation and associated macro-to-micro interfaces as the pumping force is transmitted in a contact-free fashion by the centrifugal field. The actuation unit can readily be adapted from macroscopic drives of commercially available *compact-disk* (CD) players. Flow control on rotating disks is, for instance, achieved by capillary-burst valves which are hydrophobic patches blocking a flow until a specific rotational frequency is reached.[7,8] Recently, these platforms have been employed in several "lab-on-a-disk" applications in the field of drug discovery or preanalytical sample preparation.[2,9,10]

So far, the impact of the Coriolis pseudo-force has not been considered for these centrifugal platforms despite the fact that the Coriolis force can prevail over all other forces beyond a certain speed of rotation.[11,12] In this work, we experimentally confirm the presence of a strong Coriolis force and show how this force is implemented to realize a novel concept of a flow switch.

2. Coriolis force

The hydrodynamics on rotating disks is described by the Navier–Stokes equation. The centrifugal force density

$$\vec{f}_\omega = -\rho \vec{\omega} \times (\vec{\omega} \times \vec{r}) \tag{1}$$

is experienced by a liquid of mass density ρ within a channel in radial r-direction on a disk spinning at $\omega = 2\pi v$ where v denotes the frequency of rotation (Fig. 1). The overall centrifugal force $\vec{f}_\omega$ induced on a liquid plug of length l on the disk depends on its radial position r.

The average density of the pumping force

$$\bar{f}_\omega = \frac{1}{l}\int_{r_<}^{r_>} \rho\omega^2 r\,\mathrm{d}r = \frac{1}{2l}\rho\omega^2(r_>^2 - r_<^2) = \rho\omega^2\bar{r} \tag{2}$$

of the liquid plug extending between its inner and outer radial positions $r_<$ and $r_>$, respectively, is obtained by integrating

eqn. (1) over the radial length $l = r_> - r_<$ with

$$\bar{r} = \frac{1}{2}(r_> + r_<) \tag{3}$$

as the mean radial position of the liquid.

Fluid propulsion in the radial channels on the disk is limited to the plane perpendicular to the angular velocity $\vec{\omega}$ parallel to the z-axis and thus the velocity has only the radial component $\vec{u}_r$. In order to allow a simple analytical treatment, a 2-dimensional flow through a gap of width

$$\Delta x = 2x_0 \tag{4}$$

between the walls located at $x = \pm x_0$ instead of the rectangular channels in our experiments as well as stationary and laminar flow conditions are assumed. With these
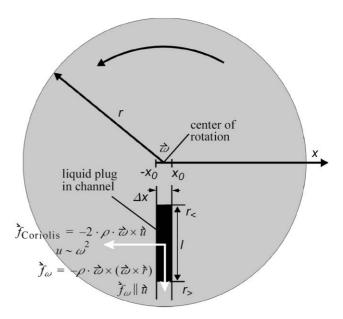

Fig. 1 A liquid plug in a channel of width $\Delta x = 2 x_0$ on a disk with radius r spinning at $\vec{\omega}$ is exposed to the radial centrifugal force f_ω (eqn. (1)). The radial position $\bar{r}$ and the length l of the plug is characterized by its boundaries $r_<$ and $r_>$. Additionally, the Coriolis force $\vec{f}_{\text{Coriolis}}$ (eqn. (7)) appearing solely in the rotating reference frame acts perpendicular to the flow velocity $\vec{u}$.

simplifications, the balance of centrifugal and viscous forces can be expressed by the inhomogeneous differential equation of second order in the azimuthal coordinate x

$$0 = -\rho \omega^2 \bar{r} - \eta \frac{\partial^2 u_r}{\partial x^2} \qquad (5)$$

with the viscosity of the liquid η. The impact of the Coriolis force (see below) on the radial flow is still discarded at this point.

Setting the flow velocity $\vec{u}$ to zero at both channel walls, $u(-x_0) = u(x_0) = 0$, a parabolic flow profile fulfills eqn. (5) with

$$u_{\text{max}} = \frac{\rho \omega^2 \bar{r}}{2\eta} x_0^2 \qquad (6)$$

representing the maximum velocity in the center of the channel (gap).

Now we investigate the Coriolis pseudo force

$$\vec{f}_{\text{Coriolis}} = -2\rho \vec{\omega} \times \vec{u} \qquad (7)$$

appearing in a non-inertial reference frame rotating at $\vec{\omega}$, *i.e.* with the disk at rest. While the transversal Coriolis force has only little impact on the so far considered radial flow, it will have a major impact on the lateral deflection of flow which is implemented for the hydrodynamic switch structure presented in this work.

This pseudo-force acts perpendicular to the plane spanned by the flow velocity $\vec{u}$ and the angular frequency of rotation $\vec{\omega}$.

The ratio

$$\frac{\left| \vec{f}_{\text{Coriolis}} \right|}{\left| \vec{f}_\omega \right|} = \frac{\rho \Delta x^2 \omega}{4\eta} \qquad (8)$$

compares the centrifugal force (eqn. (2)) in radial direction to the transversal Coriolis force (eqn. (7)) acting perpendicular to the direction of a liquid flow with viscosity η. Here the steady state at a constant frequency $d\omega/dt = 0$ without any rotational *Euler* acceleration is considered. For the liquid characteristics of water ($\rho = 10^3$ kg m^{-3}, $\eta = 0.89 \times 10^{-3}$ Pa s) and a typical channel width $\Delta x = 200$ μm, the ratio roughly amounts to $10^{-2}\omega$. This way, for frequencies beyond only $\omega_c = 100$ rad s^{-1} (≈ 16 Hz), the Coriolis force even prevails over the centrifugal force!

The force density

$$f_\Theta = \frac{p_\Theta \Delta x^2}{l \Delta x^2} = \frac{p_\Theta}{l} = \frac{4\sigma}{l \Delta x} \cos\Theta \qquad (9)$$

associated with the capillary pressure p_θ in a square channel of width and height Δx and length l is a function of contact angle Θ and surface tension σ. Both are independent of ω.

The ratio between $\vec{f}_{\text{Coriolis}}$ and $\vec{f}_\Theta$

$$\frac{\left| \vec{f}_{\text{Coriolis}} \right|}{\left| \vec{f}_\Theta \right|} = \frac{\rho^2 \Delta x^3 l \omega^3 \bar{r}}{16\sigma\eta\cos\Theta} \propto \omega^3 \qquad (10)$$

is highly dependent on ω. Inserting the values for a water plug ($\rho = 10^3$ kg m^{-3}, $\sigma = 72.5 \times 10^{-3}$ N m^{-1}, $\eta = 0.89 \times 10^{-3}$ Pa s, $l = 1$ cm, $\bar{r} = 3$ cm) and assuming a channel with fully wetting surfaces ($\Theta = 0$) and typical dimensions ($l = 1$ cm, $\Delta x = 200$ μm)

the equilibrium between both force densities is reached already at a frequency ω of about 75 rad s^{-1}. This explains the minor impact of surface related phenomena in the following experiments where frequencies far beyond this critical threshold are implemented.

3. Concept of flow switch

In this paper, the presence of a strong Coriolis effect is demonstrated by a fluidic switch that splits the flow from a common radial inlet channel *via* an inverse Y-structure into two symmetric outlets (Fig. 2). If Coriolis effects did not exist, 50% of the flow would be evenly distributed among the two outlets. However, a dominating Coriolis force induces a bias, eventually directing 100% of the flow into one particular outlet which can be addressed according to the direction of rotation.

The influence of the Coriolis force is measured by recording the filling height h_i, i {1,2} in each outlet reservoir R$_1$ and R$_2$, respectively, which are both of width w and depth d (Fig. 3). Thus, the volume

$$V_i(T) = \int_T I_i \mathrm{d}t = w d h_i(T) \qquad (11)$$

collected by each reservoir i corresponds to the integral of the volumetric flow rates I_i over the experimental period of time T. The filling heights h_i are thus proportional to the volumes V_i.

Inertial effects ("Euler force") resulting from the acceleration phase of the disk from zero rotation to a particular frequency resemble the Coriolis effect. Although this effect might be used to support the flow switching, they are ruled out by an acceleration chamber in order to attribute the flow switching solely to the Coriolis force. The acceleration chamber is situated downstream of the loading reservoir. Its volume capacity is chosen to provide an intermediate storage of liquid during the entire acceleration phase of the disk. After some time of typically 1s, when steady state conditions are established, the liquid overflows into the switch structure.

4. Experimental results

The microfluidic structures are fabricated by CNC milling in PMMA substrate of standard CD-format and sealed by an adhesive tape covering the full disk[13] (Fig. 3). The width and the depth of the incoming channel measure 360 μm and
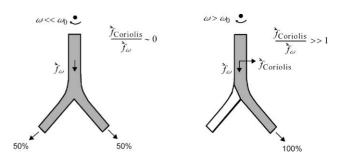

Fig. 2 Flow through a symmetric, inverse Y-structure. Left: At low frequencies $\vec{\omega}$, where the Coriolis force is negligible, the flow is divided up at similar flow rates through both outlets. Right: A dominating Coriolis force at frequencies beyond ω_0 diverts 100% of the flow into one addressable outlet according to the direction of rotation.
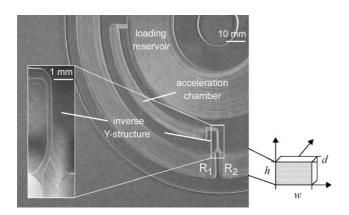
Fig. 3 Sector of the test structure milled in a PMMA disk featuring the loading reservoir, the acceleration chamber, the switch structure and the two reservoirs R_1, R_2. Left insert: Zoomed out inverse Y-structure. Right: Dimensions height h, width w, depth d of the reservoirs.

125 μm, respectively. The reservoirs and the acceleration chamber possess a depth of 900 μm. The filling heights h_i in the outlets are recorded during rotation by our designated measurement setup.[14] The setup is composed of a modified compact-disc player (Bio-Disk player[5]), a microscope (Leica MZ 12.5, Leica Microsystems GmbH[15]) mounted on a camera with a 100 ns minimum exposure time (Sensicam fast shutter 370 KF 3411, PCO Computer Optics GmbH[16]) and a stroboscopic flash (Drelloscope 255-01, Drello GmbH[17]). The camera and the flash are periodically triggered by the zero crossing signal of the rotating disk to capture the transient filling heights $h_i(t)$ in the two reservoirs.

Experimental investigations of the switch structure clearly show that above a threshold frequency $\omega_0 = 350$ rad s^{-1} (~ 55.7 Hz), the entire flow is diverted into one designated outlet channel defined by the direction of rotation (Fig. 4). Since acceleration effects are ruled out by the intermediate acceleration chamber, the switching of flow solely results from the transversal Coriolis force.

5. CFD simulations

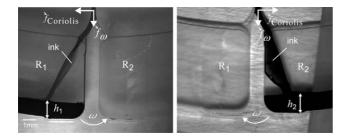To investigate the impact of the Coriolis force on the switching behaviour, extensive numerical simulations have been carried out using the commercial code ACE+ from CFDRC (*CFD-GUI -Revision* 2002.2.16, *CFD-ACEU solver-Revision* 2002.0.40[18]). The inverse Y-structure without any reservoirs is simulated in a reference frame rotating at the same speed as the disk, *i.e.*, with the channels remaining at rest. The 3-dimensional simulations are carried out under steady-state conditions with fixed-pressure boundary conditions at inlets and outlets and no-slip condition at the walls. The structure is also completely filled by liquid to avoid liquid–air interfaces which would significantly raise the numerical complexity of the simulation. The experimental observations are supported by the simulated velocity profile depicted in Fig. 5.

6. Switching characteristic

Fig. 6 shows a sequence of the switching operation at a frequency of 350 rad s^{-1}. Monitoring both reservoirs shows the exact switching of liquid into only one addressed reservoir. There is no liquid entering the other reservoir at any time over the whole course of switching.

In order to quantify the switching characteristic below the threshold frequency ω_0, the ratio $\gamma \approx h_2/h_1$ of the measured filling heights h_1, h_2 is taken at different frequencies between 75 rad s^{-1} (~ 12 Hz) and 350 rad s^{-1} (~ 55.7 Hz) (Fig. 7).
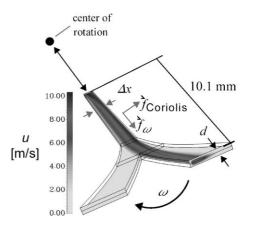

Fig. 5 Simulated flow velocities in the inverse Y-structure ($\Delta x = 360$ μm, depth $d = 125$ μm) at $|\bar{\omega}| = 350$ rad s^{-1}. The flow distribution between both outlets shows that more than 90% of the flow is diverted into the right outlet by the Coriolis force.
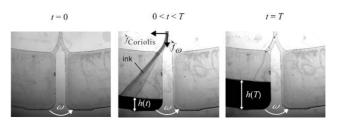

Fig. 4 Switched flow at $|\omega| = 350$ rad s^{-1}. Left: Segment showing the outlets on the disk rotating counterclockwise. Ink streams solely into the left reservoir which is addressed by the direction of rotation. The other reservoir remains unaffected. Right: Segment showing the situation for clockwise rotation. According to the direction of rotation ink streams only into the right reservoir.

Fig. 6 Sequence of flow switching at $\omega = 350$ rad s^{-1} at different times t. Left: At a time $t = 0$ before the liquid reaches the switch, both reservoirs are empty. Middle: At an intermediate time $0 < t < T$, the ink is deviated into the left reservoir according to the direction of the Coriolis force. Right: At $t = T$, the entire plug is collected in the left reservoir. The other reservoir remains empty.
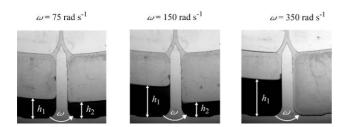
ω = 75 rad s⁻¹   ω = 150 rad s⁻¹   ω = 350 rad s⁻¹

Fig. 7 Measured filling heights h_1 and h_2 in both reservoirs after experimental time T at different frequencies ω. The used liquid is ink. Left: Similar filling heights in both reservoirs at ω = 75 rad s⁻¹ (differences result from geometric tolerances in the channel due to the milling process). Middle: At a frequency ω = 150 rad s⁻¹ (counterclockwise rotation), a clear shift of the filling heights towards the left reservoir is evident. Right: At frequencies ω = 350 rad s⁻¹, the entire liquid volume is filled into the left reservoir.

At frequencies below 75 rad s⁻¹ ($\sim$12 Hz), the Coriolis force is negligible and the flow rates I_i and filling heights h_i are nearly equal. Towards higher frequencies, the filling heights change according to the increasing force $\vec{f}_{\text{Coriolis}}$ until the complete flow is diverted into one channel above 350 rad s⁻¹ ($\sim$55.7 Hz). Note that the error due to the rounded edges in the experimental chambers with respect to eqn. (11) where a rectangular chamber is assumed is negligible as the ratio of the azimuthal extension of the reservoirs is about 15 times greater than their height.

Due to symmetry, changing the direction of rotation diverts the flow into the other reservoir. The experimental filling ratios γ are in excellent agreement with simulated flow ratios of the outlets (Fig. 8). The deviations at low frequencies are related to small asymmetries of the inverse Y-structure resulting from tolerances in the micromilling process. The differences between
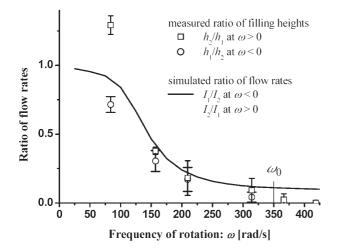

Fig. 8 Ratios of measured filling heights h_1, h_2 and simulated flow rates I_i at the outlets over frequency of rotation ω in both rotational directions represented by $\omega > 0$ (counterclockwise) and $\omega < 0$ (clockwise). The ratio of flow rates at frequencies below 75 rad s⁻¹ ($\sim$12 Hz) shifts from 1.0 to nearly 0 towards higher frequencies due to an increasing Coriolis force. Beyond 350 rad s⁻¹ ($\sim$55.7 Hz), the ratio amounts to 0 since the entire flow is diverted into one outlet. Deviations of the simulations from the experiment at low frequencies result from the fabrication process.
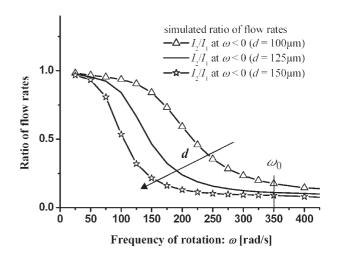

Fig. 9 Simulated ratio of flow rates I_i over frequency of rotation $\omega > 0$ at different channel depths d. The threshold frequency ω_0 of the flow switching can be tuned by changing the channel dimension since a lower hydrodynamic resistance in the switch structure leads to a higher flow velocity and a stronger Coriolis force.

experiments and the corresponding simulation at frequencies beyond 350 rad s⁻¹ where complete flow switching is experimentally observed, can be explained by the neglect of any interfacial effects in the CFD-model.

Simulations in Fig. 9 show that the threshold frequency ω_0 strongly depends on the channel depths d, since the velocity profile and thus $\vec{f}_{\text{Coriolis}}$ scales with d^2. An increase of d results in a lower hydrodynamic resistance of the Y-structure, leading to a higher velocity for a particular frequency. This corresponds to a shift of ω_0 towards smaller values.

7. Conclusion and outlook

We used the Coriolis pseudo force in a rotating radial microchannel to design a flow control element that apportions an incoming stream between two symmetric outlets. Beyond a frequency threshold which is a function of the channel geometry, the flow is completely diverted into one particular outlet selected by the sense of rotation. Frequency thresholds in the range 30–50 Hz are found for the typical microfluidic conditions examined in this work. These experiments comply with our accompanying CFD simulations.

Our investigations prove that the apparent Coriolis force can be employed to regulate flow on fast spinning lab-on-a-disk platforms. One aspect of particular interest is that the Coriolis force is perpendicular to the velocity, *i.e.* the radial direction in microfluidic channels. Thus, the axisymmetic, *i.e.* 1-dimensional motion of the disk in the lab frame translates into a 2-dimensional hydrodynamic force on the moving liquid in the non-inertial disk frame. We currently explore how to implement the 2-dimensional force for a hydrodynamic patterning of flow.

Thilo Brenner, Thomas Glatzel, Roland Zengerle and Jens Ducrée
IMTEK—University of Freiburg, Laboratory for MEMS Applications, Georges-Koehler-Allee 106, D-79110 Freiburg, Germany. www.imtek.de/anwendungen; E-mail: tbrenner@imtek.de

References

1 M. J. Madou and G. J. Kellogg, LabCD: A centrifuge-based microfluidic platform for diagnostics, *Proceedings of SPIE*, 1998, vol. **3259**, pp. 80–93.

2 D. C. Duffy, H. L. Gillis, J. Lin, N. F. Sheppard and G. J. Kellogg, Microfabricated Centrifugal Microfluidic Systems: Characterisation and Multiple Enzymatic Assays, *Anal. Chem.*, 1999, **71**, 20, 4669–4678.

3 M. J. Madou, L. J. Lee, S. Daunert, S. Lai and C. Shih, Design and Fabrication of CD-like Microfluidic Platforms for Diagnostics: Microfluidic Functions, *Biomed. Microdev.*, 2001, **3:3**, 245–254.

4 G. Thorsén, G. Ekstrand, U. Selditz, S. R. Wallenborg and P. Andersson, Integrated Microfluidics for Parallel Processing of Proteins in a CD Microlaboratory, *Proceedings of Micro Total Analysis Systems*, MESA Monographs, 2003, pp. 457–460.

5 J. Ducrée and R. Zengerle, Bio-Disk: A centrifugal platform for integrated point-of-care diagnostics on whole blood, http://www.bio-disk.com.

6 FlowMap—Microfluidics Roadmap for the Life Science, ed. J. Ducrée and R. Zengerle, Books on Demand, Norderstedt, Germany, ISBN 3-8334-0744-1, http://www.microfluidics-road-map.com.

7 G. Ekstrand, C. Holquist, A. Örlefors, B. Hellman, A. Larsson and P. Andersson, Microfluidics in a Rotating CD, *Proceedings of Micro Total Analysis Systems*, Kluwer Academic Publisher, Dordrecht, The Netherlands, 2000, pp. 311–314.

8 J. Zing, D. Bannered, M. Desponded, J. Gilbert, D. C. Duffy and G. J. Kellogg, Design analyses of capillary burst valves in centrifugal microfluidics, *Proceedings of Micro Total Analysis Systems*, Kluwer Academic Publisher, Dordrecht, The Netherlands, 2000, pp. 579–582.

9 M. J. Madou, Y. Lu, S. Lai, C. Koh, L. J. Lee and B. R. Wenner, A novel design on a CD disc for 2-point calibration measurement, *Sens. Actuators A*, 2001, **91**, 301–306.

10 M. Inganäs, G. Ekstrand, J. Engström, A. Eckersten, H. Dérand and P. Andersson, Quantitative Bio-affinity Assays at Nanoliter Scale, Parallel Analysis of Crude Protein Mixtures, *Proceedings of Micro Total Analysis Systems*, Kluwer Academic Publisher, Dordrecht, The Netherlands, 2001, pp. 91–92.

11 T. Brenner, T. Glatzel, R. Zengerle and J. Ducrée, A flow switch based on Coriolis force, *Proceedings of Micro Total Analysis Systems*, MESA Monographs, 2003, pp. 603–606.

12 J. Ducrée, T. Brenner, T. Glatzel and R. Zengerle, A Coriolis-based split-and-recombine laminator for ultrafast mixing on rotating disks, *Proceedings of Micro Total Analysis Systems*, MESA Monographs, 2003, pp. 903–906.

13 Jobst Technologies, Stefan-Meier-Strasse 8, 79114 Freiburg, Germany, http://www.jobst-technologies.com.

14 T. Brenner, M. Grumann, C. Beer, R. Zengerle and J. Ducrée, Microscopic Characterisation of Flow Patterns in Rotating Microchannels, Proceedings of MICRO.tec, Munich, Germany, October 2003, pp. 171–174.

15 Leica MZ 12.5, Leica Microsystems GmbH, 64624 Bensheim, Germany, http://www.leica-microsystems.com.

16 PCO Computer Optics GmbH, 93309 Kehlheim, Germany, http://www.pco.de.

17 Drello GmbH & Co KG, 41179 Moenchengladbach, Germany, http://www.drello.de.

18 CFD Research Corperation, 215 Wynn Drive, Huntsville, Alabama 35805, USA, http://www.cfdrc.com.